Surface Science 275 (1992) 414–423
North-Holland

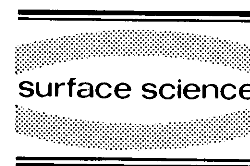

In situ STM observations of the etching of n-Si(111) in NaOH solutions

Philippe Allongue [1], Harald Brune and Heinz Gerischer
Fritz-Haber-Institut der Max-Planck-Gesellschaft, Faradayweg 4–6, D-1000 Berlin 33, Germany

Received 27 January 1992; accepted for publication 25 May 1992

In situ scanning tunneling microscopy (STM) has been used to investigate the bias dependence of the etching of Si(111) in alkaline solutions. Sequences of images showing the time evolution of the surface structure have been recorded. Under hydrogen evolution, double layer steps (~ 3 Å) are preferentially etched laterally. Closer to the rest potential, corrosion pits (~ 3 Å deep, i.e., one Si double layer deep) are nucleated on wider terraces, increasing the etch rate. Individual atoms could also be resolved on terraces, showing that the surface of Si(111) is unreconstructed when in contact with an aqueous solution. The results presented here confirm previous electrochemical data concerning the bias dependence of the etch rate and yield new insight into the etch mechanism of Si in such solutions.

1. Introduction

Many studies of solid surfaces in contact with electrolytes by in situ application of scanning tunneling microscopy (STM) or atomic force microscopy (AFM) have been made on noble metal single crystals, and atomic resolution has been achieved in the last two years by several groups. The structure of underpotential-deposited metal films [1–5], layers of adsorbates [5–7] and the reconstruction of a gold surface [8,9] have been analyzed in this way. Semiconductor surfaces in contact with electrolytes have also been investigated by STM [10–16]. However, it appears much more difficult to obtain there in situ atomic resolution, particularly in the case of reactive semiconductors such as GaAs or Si. Only very recently monatomic steps have been seen on silicon in H_2SO_4 solution after etching in HF [17] or in NH_4F solutions of intermediate pH [18,19].

Etching of Si in alkaline solutions is very orientation-dependent [20,21], a property which finds many applications in industry. This process has been investigated by several groups from an electrochemical point of view [22–25]. These studies have concluded that the rate-determining step is of chemical nature (no free electronic charge carrier involved) and that it can be stopped under cathodic polarization. However, this bias dependence of the etch rate of n-Si seems in conflict with a purely chemical description of the reaction and still needs an explanation. One group has attributed the cathodic etch stop to the presence of an intermediate layer of "incomplete etch products" detected by ellipsometry [23]. Such questions should be easily clarified by STM studies.

In this paper we report the first in situ STM observations of n-type Si(111) surfaces during the etching process in NaOH solutions: we were able to follow the lateral etching of Si double layer steps (~ 3 Å high) on the surface and achieved atomic resolution on terraces between steps.

2. Experimental

STM observations were performed in the electrolytic environment with a pocket-size STM cou-

[1] Permanent address: LP 15 CNRS, Laboratoire de Physique des Liquides et Electrochimie, 4 Place Jussieu, F-75005 Paris, France.

0039-6028/92/$05.00 © 1992 – Elsevier Science Publishers B.V. All rights reserved

pled with a potentiostat. The electronics of the STM are described in ref. [1]; the conversion factor of the I/V converter used here is 10^8 V/A. The STM itself is a new design utilizing a piezoelectric scanner tube which was laterally and vertically calibrated by imaging graphite and Au(111), respectively. W tips were prepared by electrochemical etching in a 2M NaOH solution. They were subsequently coated with apiezon wax leaving the very end exposed. To further minimize the faradaic current, the tip potential could be accordingly adjusted with respect to the reference electrode, independently of the sample polarization (4 electrode configuration). The reference electrode was a Pd wire loaded with hydrogen by evolving H_2 for ~ 30 min ($I \sim 10$ mA) in a 1M NaOH solution. The potential of the reference electrode, hereafter denoted Pd–H, was fairly stable against a saturated calomel electrode (SCE) over several hours after a slow drift of about 50 mV during the first two hours. This reference electrode potential corresponds to -1.0 V/SCE.

Relatively low-doped (10 $\Omega \cdot$ cm) n-type Si(111) samples (purchased from Siltronix-France) with a 1.2° miscut angle were employed in this work. Prior to experiment, samples were cleaned in trichlorethylene, acetone and methanol, then rinsed in triply distilled water and subsequently etched in a 40% NH_4F solution for ca. 6 min in order to start with an ideally H-terminated surface [26,27]. Solutions were prepared with reagent grade chemicals and triply distilled water.

All STM observations correspond to the constant current mode, with tunneling currents in the range 0.2–0.5 nA. The x-scan frequency was in the range 2–6 Hz, and images were recorded within times ranging between 40 and 70 s. All images correspond to raw data with the exception of an adjustment of the background plane and/or the use of different coloring processings. No filtering of images has been performed.

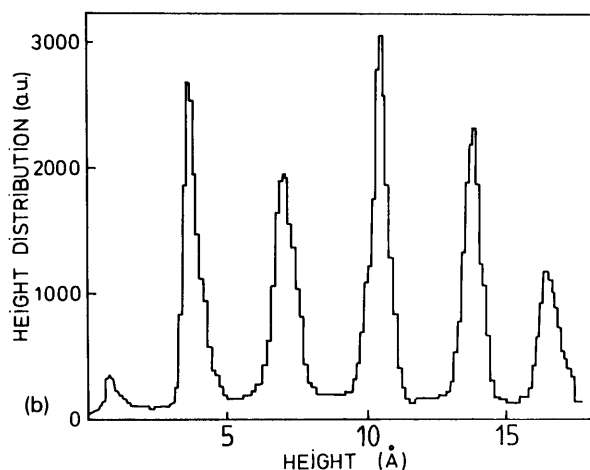

Fig. 1. (a) In situ STM observation of the surface of n-Si(111) in 2M NaOH under relatively strong hydrogen evolution. Tunneling conditions: sample: $U_S = -0.58$ V/Pd–H; $I_S = -200$ μA/cm^2; tip: $U_T = 0.02$ V/Pd–H; $I_T = 0.2$ nA. The frame is 1280×1470 Å^2. Terraces go upwards from bottom left to upper right. (b) Distribution of heights after adjustment of the background plane so as to make terraces horizontal. Each terrace is separated by a single double layer.

3. Results

Fig. 1 is a general view of the surface of n-Si(111) in contact with a 2M NaOH solution under cathodic polarization. The cathodic current associated to the hydrogen evolution did not interfere with the imaging up to densities of 1

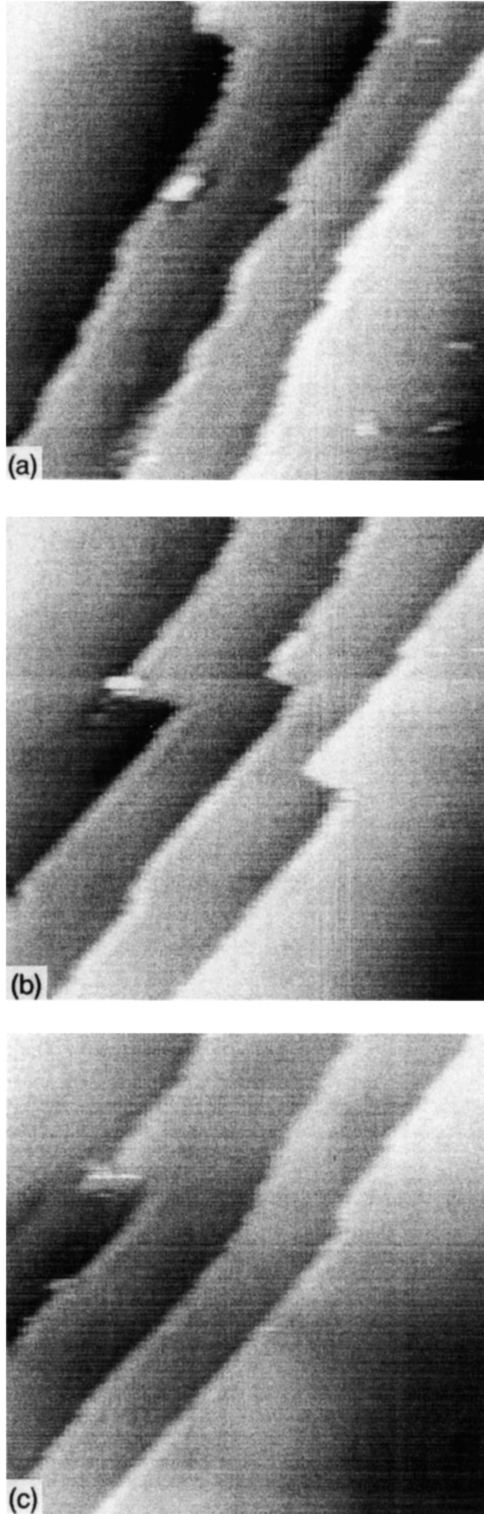

Fig. 2. Sequence of STM images showing the evolution of step edges on an n-Si(111) surface in contact with 2M NaOH. The (380×380 Å^2) images (a–c) have been recorded in 45 s. The time elapsed between images is 90 s. Tunneling conditions: sample: $U_S = -0.63$ V/Pd–H; $I_S = -150$ μA/cm^2; tip: $U_T = +300$ mV/Pd–H; $I_T = 0.2$ nA.

mA/cm^2. Such high currents made however imaging difficult after some time because of a too strong generation of gas bubbles with respect to the small dimensions of the cell. This image shows that the surface consists of smooth terraces, with a step height close to the 3.14 Å expected for a double layer step on Si(111), within the calibration accuracy of the piezoelement. Terrace edges present a sawtooth-like shape containing many kinks. Angles between terrace edges are often different from the expected 60° and the terrace widths are not uniform (with a miscut angle of 1.2°, terraces are expected to be about 150 Å wide). Such large scale images displayed minor modifications with time and looked stable. They could be recorded only if the silicon remained cathodically polarized. This observation is consistent with the existence of a cathodic etch stop at n-Si [24,25]. If the electrode was kept at the rest potential for a too long time, terraces became much smaller and the overall surface looked much rougher with hillocks of many double layers high, consistent with the state of the surface after a long period of etching [23].

Focusing on a smaller area, structural changes can be seen in more detail. Fig. 2 presents a series of 3 STM images recorded every 90 s on the same area. The H_2 current is similar to that in fig. 1. The white spot (probably an impurity) serves as a point of reference to account for the thermal drift between frames. This portion of the surface was interesting, since steps are relatively smooth compared to other parts of the surface. In fig. 2a the three steps (one Si double layer high) are almost parallel and rectilinear and terraces go downwards from right to left. In fig. 2b, a strip of material (~ 40 Å wide) has been dissolved at the three terrace edges, as evidenced by the corners generated on step edges. The three corners moved from the lower left side of the

images towards the upper right. This demonstrates, in almost real time, that etching proceeds by a step flow mechanism at this potential. The process continues between figs. 2b and 2c for the two upper steps while the motion of the corner on the lowest terrace edge has been pinned by an impurity on the etch line. Note that the etching has resulted locally in perfectly smooth steps which must be parallel to the [110] direction since steps corresponding to (111) microfacets are the less reactive. Observations on other places have confirmed that the flow and the smoothing of steps critically depends on their initial shape, i.e., on the presence of defects.

At a cathodic potential 0.2 V closer to the open circuit potential (OCP is about 0 V/Pd–H), the hydrogen current decreases to 40 $\mu A/cm^2$ and the surface becomes more reactive, as shown by the series of STM images of fig. 3 (images have been recorded every 90 s). A larger area

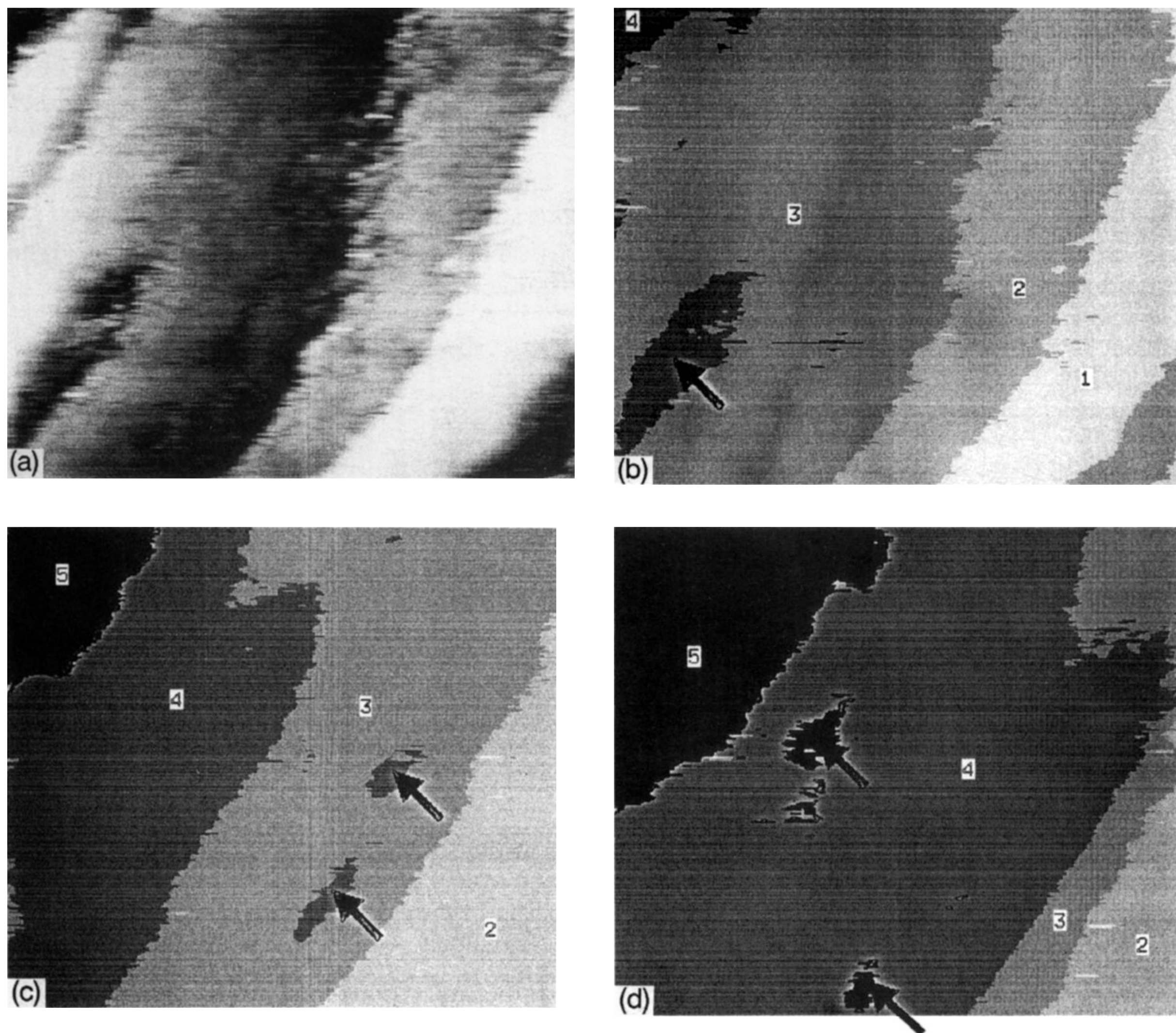

Fig. 3. Same as fig. 2 for a weaker hydrogen evolution rate. Tunneling conditions: sample: $U_S = -0.4$ V/Pd–H; $I_S = -40$ $\mu A/cm^2$; tip: $U_T = 0.04$ V/Pd–H; $I_T = 0.4$ nA. Images (a) and (b) correspond to the same area with different shading (see text). The (900 × 780 Å^2) images (b–d) have been recorded in 45 s. The time elapsed between images is 90 s. The same index and color is conserved for each terrace over the whole series.

than in fig. 2 had to be observed in order to follow the structural changes since these were much faster than before. In fig. 3a (classical grey scale representation) the image appears more fuzzy than in figs. 1–2 which might reflect the surface instability, especially at step edges. Such sequences were also difficult to observe over long periods because the tip generally lost its resolution after a while. To facilitate the viewing of the process, each terrace (one double layer high) has been characterized by an index and a color which are conserved over the whole series (steps go downwards from white to black). Figs. 3a and 3b compare images of the same area utilizing the two shading processes. At this potential, a corrosion pit (one double layer deep) is visible on the largest terrace (terrace 3); its growth is so fast towards the downward terrace edge that half of terrace 3 has already disappeared in fig. 3c. A similar process with pit formation and growth can also be seen between figs. 3c and 3d. Besides this main process, a slower motion of other step edges can also be noted.

The nucleation of *new* etch pits on terraces could not be seen at more negative potentials which explains the cathodic etch stop on n-Si [25,26]. However, the growth of *pre-existing* pits cannot be completely prevented, even under the electrochemical conditions of figs. 1–2 (hydrogen current of 200 $\mu A/cm^2$). In fig. 4a, the triangular etch pits have been created by shortly polarizing the sample as in fig. 3 and stepping back the potential negatively. Focusing on the lower half of the area, figs. 4b–4f present a sequence of images recorded every 50 s. The growth of *initially triangular* pits (one double layer deep) and their coalescence can be observed while in the mean time no nucleation of new pits occurs. This series visualizes why terrace edges do not systematically correspond to (111) microfacets if one considers the evolution of the two pits indexed by an arrow: the crystallographic directions are lost after some time. Even in the case of isolated pits, observations showed that their triangular shape disappears if their growth is fast, as in fig. 3, or if their size exceeds a critical size.

Finally, fig. 5 presents a high resolution in situ STM image recorded on a terrace. The solution was 1M NaOH. This is the first time, to our knowledge, that individual atoms are resolved on a silicon surface contacting a solution. Keeping atomic resolution over large areas was difficult because of changes at the W tip. Terraces appear atomically ordered with an atom spacing close to the 3.84 Å expected for a (1 × 1) unreconstructed Si(111) surface. The corrugation in fig. 5 is about 0.2 Å, a value which is close to the 0.5 Å reported by Hessel et al. [28] in UHV-STM observations of etched Si(111). Higashi et al. [29] reported a corrugation of only 0.03 Å. The observation of fig. 5 is consistent with UHV studies which show that a surface of Si(111), covered with hydrogen by wet chemical etching, exhibits a well-ordered (1 × 1)-H structure [28–30]. Since LEED studies show that in the UHV water adsorption on Si(111) lifts off the (2 × 1) reconstruction to yield also the (1 × 1) unreconstructed structure [31,32], it is not possible to ascertain the nature of surface ligands

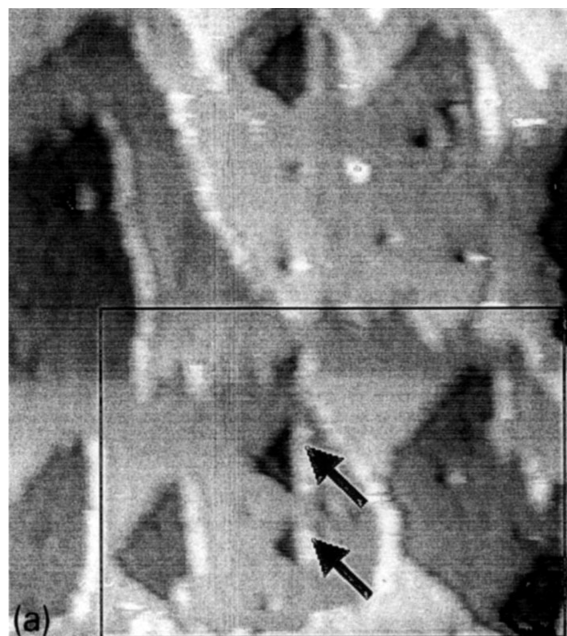

Fig. 4. Same as in fig. 1. (a) General view (1076 × 1193 Å^2); (b–f) time evolution of the lower half of the surface (860 × 570 Å^2). Before recording this sequence the sample has been polarized close to the OCP to create the initially triangular etch pits. The hydrogen current is 200 $\mu A/cm^2$. The time elapsed between images is 50 s.

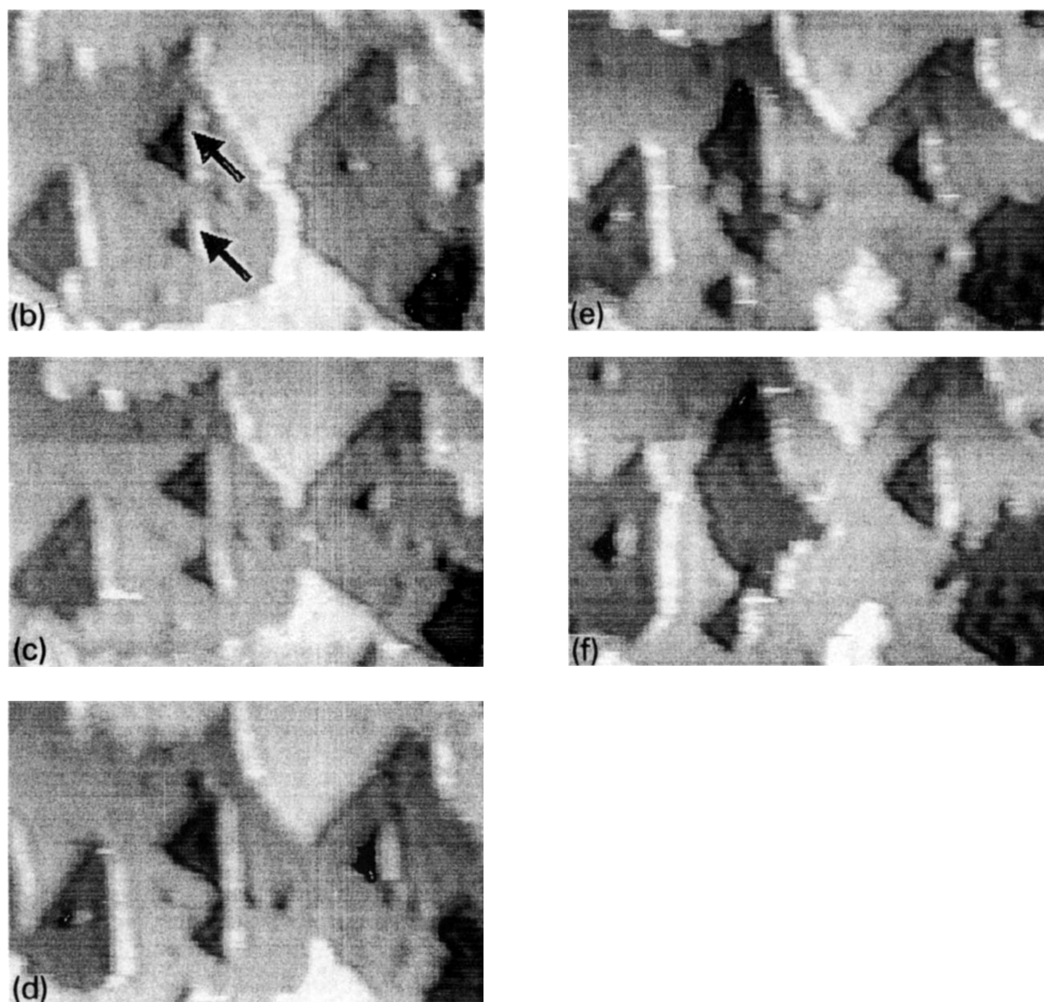

Fig. 4. Continued.

from fig. 5. However, given the relative hydrophobic character of the surface after etching, it is suggested that under cathodic polarization the surface is mostly covered with hydrogen, particularly on terraces, and that OH groups may only exist at step edges.

4. Discussion

The STM results of figs. 2 and 4 demonstrate that the etching of Si(111) faces in NaOH is dominated by a step flow mechanism. This process competes with the nucleation of etch pits on terraces when the potential approaches the OCP (fig. 3). Note, however, that the etch pits are always one double layer deep, consistent with the much slower etch rate measured in the (111) direction in NaOH solutions [20,21]. This explains that the etching is essentially lateral.

Due to this layer by layer etching process, one can tentatively evaluate an overall etch rate from the displacement of the layer edges of the silicon in figs. 2–4. Measuring the surface of terraces which have been removed in the sequences of images, dividing it by the time elapsed and normalizing the ratio to the total surface of the observed area, one obtains the number of layers

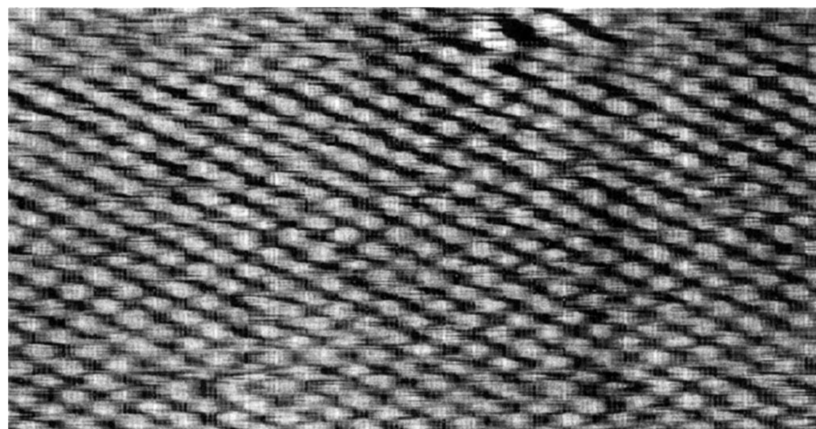

Fig. 5. Atomically resolved in situ STM image of n-Si(111) in 1M NaOH. Tunneling conditions: sample: $U_S = -0.54$ V/SCE; $I_S = -40$ μA/cm^2; tip: $U_T = 0.15$ V/Pd–H; $I_T = 0.5$ nA. The atomic corrugation is about 0.2 Å. The frame is 103×54 Å^2. The representation is such that the surface is illuminated from the left.

removed per unit of time. Taking 3.14 Å as step height, one finds a local etch rate of about 0.2, 1.4 and 0.16 Å/min under the electrochemical conditions of figs. 2, 3 and 4, respectively. These values are quite consistent with etch rate determinations found in the literature [23,24] for comparable conditions of polarization and confirm that the etch almost stops cathodically.

The general aspect of the surface topography results from the ratio between the rate of the etch pit formation and that of the step flow. If the second mechanism is much faster than the first one and/or the miscut angle increases, newly formed pits have no time to grow and the initial spacing between steps (as given by the miscut angle) will be conserved. Conversely an increase of the rate of the pit formation will make the movement of terrace edges irregular as it is illustrated in fig. 4. Hessel et al. [28] recently studied the etching of Si(111) in NH_4F solutions of intermediate pH. By transferring the samples into the UHV for STM observations, the authors concluded that the etching of Si is a step flow mechanism in solutions of pH > 7 since the initial mean distance between double layer steps was conserved. The etch rate of silicon in aqueous NaOH is higher than in NH_4F solutions [33] presumably because of an easier nucleation of pits on terraces in the former solution (see fig. 3). This would explain that the topography of the surface (fig. 1) is different from that found after etching in NH_4F, although the samples used here were also pretreated in NH_4F prior to observations. Indeed, before images could be obtained, it must be kept in mind that samples stayed probably enough time in contact with the NaOH solution to create a surface structure characteristic of this etch.

With regard to the etching mechanism it is important to note that the hydrogen evolution reduces the corrosion rate (figs. 2–4) in agreement with literature data [24], but does not stop it *completely* even for a cathodic current of 200 μA/cm^2. This suggests an intimate coupling between the electrochemistry of the hydrogen evolution and that of the corrosion. Here we shall refrain from a detailed analysis of the electrochemical processes. This will be done in another paper together with the presentation of some electrochemical experiments regarding this question. Here we only want to point out at which step both processes are coupled.

Given the hydrophobic character of the surface and its atomically ordered (1×1) structure (fig. 5), it seems realistic to think that the surface of the silicon is passivated by Si–H bonds as in fluoride solutions. The H atoms are immobile and so strongly bonded to the surface that recom-

bination of two neighboring H atoms to form H_2 molecules is impossible at room temperature. Under cathodic bias, conduction band electrons are available at the surface and the only mechanism for the formation of hydrogen molecules is the so-called electrochemical desorption or Heyrovski reaction [34]. This can occur on a terrace according to the following reactions, in which $\equiv$ Si means a Si atom triply bonded to the crystal:

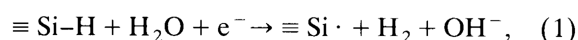

$$\equiv \text{Si–H} + H_2O + e^- \rightarrow \equiv \text{Si} \cdot + H_2 + OH^-, \quad (1)$$

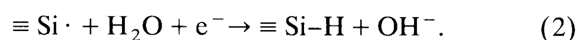

$$\equiv \text{Si} \cdot + H_2O + e^- \rightarrow \equiv \text{Si–H} + OH^-. \quad (2)$$

The net reaction of eqs. (1) and (2) produces only one H_2 molecule leaving intact the surface since reaction (2) reconstructs the initial structure $\equiv$ Si–H.

The intermediate $\equiv \text{Si} \cdot$ with an unpaired electron is very reactive. There is a chance that it reacts with water forming a $\equiv$ Si–OH bond and injecting an electron into the conduction band.

$$\equiv \text{Si} \cdot + H_2O \rightarrow \equiv \text{Si–OH} + e^- + H^+. \quad (3)$$

Increasing the negative bias (i.e., increasing the electron concentration) increases the rate of reaction (2) and makes reaction (3) less probable. If we assume that the reaction (3) is required as an initial step for the formation of etch pits on the terraces [33], since Si–Si backbonds are now weakened by the large electronegativity difference between Si and OH [33], we can understand that the rate of the etch pit formation decreases with cathodic biases. This description explains also the decrease of the overall corrosion rate with cathodic bias.

The lateral etching observed in figs. 2–4 indicates that kink sites can be easily nucleated on step edges even for cathodic polarizations. The kink site atoms have only two bonds to the crystal lattice while the two other bonds will have reacted with components of the electrolyte. The relative passivity of the silicon against corrosion at very cathodic bias (the etch rate is about 0.2 Å/min) suggests that the kink site atoms are also mostly passivated by hydrogen atoms and that hydrogen evolution equally occurs at kink sites. Hence reactions similar to the reactions (1) and (2) can be written with the $=SiH_2$ entity in the place of $\equiv$ Si–H at the beginning. A reaction analogous to reaction (3) will create a =SiHOH intermediate which we consider as necessary for the further dissolution of the kink. Such process will occur at kink sites much more frequently than on terraces. The two Si–Si backbonds of a kink site atom are also certainly weaker than in the case of terrace atoms since the polarization of the Si–OH bond is distributed over only 2 bonds instead of 3. This explains that the kink site atoms are quickly further removed from the lattice by consecutive chemical steps. The nucleation of etch pits on terraces is also therefore a much rarer event since it may need two or three $\equiv$ Si–OH configurations in immediate contact to each other.

Another argument concerns the strength of Si–H bonds. The smaller wave number of Si–H monohydrides with respect to silicon di- and trihydrides in IR spectroscopy characterizations [27] indicates that Si–H bonds on terraces are stronger than at step edges. Therefore, the formation of a radical $\equiv \text{Si} \cdot$, triply bonded to the lattice (reaction (1)) will require a higher surface electron density than at step edges. This favors the hydrogen evolution at kink sites and with it the lateral dissolution through the electrochemical coupling of reactions (1)–(3).

In this model the cathodic etch stop is caused by the dominance of step (2) over step (3). This is due to the high activity of electrons on the surface at high enough cathodic bias which prevents the nucleation of etch pits. The same competition between the formation of the $=SiH_2$ or =SiHOH structure occurs at kink sites. The complete dissolution mechanism requires a discussion of the steps consecutive to reaction (3) which concern the removal of Si atoms from kink sites or terraces. This involves several chemical reaction steps, like the hydrolyzation of polarized Si–Si backbonds by water molecules forming new Si–H and Si–OH bonds [33]. Reactions (1–3) only describe the electrochemical coupling between the hydrogen evolution and the etching processes under cathodic polarization. Note already that the hydrolyzation of the Si–H to form Si–OH, as a result of reactions (1) and (3), involves no net electron flow and goes without an external cur-

rent at open circuit. We have indications that a purely chemical hydrolyzation can compete with the electrochemical mechanism above, presumably according to the following reaction [26]:

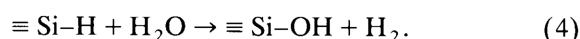

$$\equiv \text{Si–H} + H_2O \rightarrow \equiv \text{Si–OH} + H_2. \quad (4)$$

This reaction is catalyzed by OH^- and recalls the well-known fact that Si hydrides are unstable at such a high pH [35,36]. This will be discussed in a forthcoming paper.

5. Conclusion

In situ STM observations of n-Si(111) surfaces under etching conditions in NaOH solution at negative bias have demonstrated that a step flow mechanism dominates the dissolution of the crystal. Atomic resolution was achieved and indicated that the terraces have the (1×1) unreconstructed structure. The decrease of the rate of corrosion with increasing cathodic bias is explained by a coupling between the hydrogen evolution reaction and the dissolution of silicon. It is suggested that this coupling occurs by surface radicals Si · which are intermediary in the reaction of H_2 formation at cathodic biases.

Acknowledgements

P.A. gratefully acknowledges a grant of the Alexander von Humboldt-Foundation. The authors are indebted to Professor R.J. Behm (Munich University) for stimulating discussions and providing the electronic design of the STM and to Professor G. Ertl for his support of the project. Thanks are due to the electronics group of the Physical Chemistry Department, G. Heyne and K. Ruda. This work was in part supported by the Fonds der Chemischen Industrie.

References

[1] O.M. Magnussen, J. Hotlos, R.J. Nichols, D.M. Kolb and R.J. Behm, Phys. Rev. Lett. 64 (1990) 2929.
[2] C.-H. Chen, S.M. Vesecky and A.A. Gewirth, J. Am. Chem. Soc., in press.
[3] S. Manne, P.K. Hansma, J. Massie, V.B. Elings and A.A. Gewirth, Science 215 (1991) 183.
[4] T. Hachiya, H. Honbo and K. Itaya, J. Electroanal. Chem. 315 (1991) 275;
K. Sashikata, N. Furuya and K. Itaya, J. Electroanal. Chem. 316 (1991) 361.
[5] S.-L. Yau, C.M. Vitus and B.C. Schardt, J. Am. Chem. Soc. 112 (1990) 3677.
[6] S.-L. Yau, X. Gao, S.C. Chang, B.C. Schardt and M.J. Weaver, J. Am. Chem. Soc. 113 (1991) 6049.
[7] R. Vogel, I. Kamphausen and H. Baltruschat, Ber. Bunsenges. Phys. Chem., in press.
[8] X. Gao, A. Hamelin and M.J. Weaver, Phys. Rev. B 44 (1991) 10983; Phys. Rev. Lett. 67 (1991) 618.
[9] O.M. Magnussen, J. Hotlos, D.M. Kolb and R.J. Behm, Int. Conf. on STM, Interlaken, 1991, Abs. 1/C1.
[10] R. Sonnenfeld, J. Schneir, B. Drake, P.K. Hansma and D.E. Aspnes, Appl. Phys. Lett. 50 (1987) 1742.
[11] K. Itaya and E. Tomita, Surf. Sci. 219 (1989) L515; Chem. Lett. 285 (1989).
[12] T. Thundat, L.A. Nagahara and S.M. Lindsay, J. Vac. Sci. Technol. A 8 (1990) 539.
[13] E. Tomita, N. Matsuda and K. Itaya, J. Vac. Sci. Technol. A 8 (1990) 534.
[14] M. Szklarczyk, A. Gonzalez-Martin, O. Velev and J. O'M. Bockris, Surf. Sci. 237 (1990) 305.
[15] K. Sakamaki, K. Hinokuma, K. Hashimoto and A. Fujishima, Surf. Sci. Lett. 237 (1990) L383.
[16] S. Eriksson, P. Carlsson, B. Holmström and K. Uosaki, J. Electroanal. Chem. 313 (1991) 121.
[17] R. Houbertz, U. Memmert and R.J. Behm, Appl. Phys. Lett. 58 (1991) 1027.
[18] R. Houbertz, A. Hornsteiner, H.E. Hessel, U. Memmert and R.J. Behm, Int. Conf. on STM, Interlaken, 1991, Abs. 3H/116.
[19] P. Allongue, V. Kieling and H. Gerischer, Int. Conf. on STM, Interlaken, 1991, Abs. 3H/115.
[20] D.L. Kendall, Appl. Phys. Lett. 26 (1975) 195.
[21] H. Seidel, L. Csepregi, A. Heuberger and H. Baumgärtel, J. Electrochem. Soc. 137 (1990) 3612, 3626.
[22] J.W. Faust, Jr. and E.D. Palik, J. Electrochem. Soc. 130 (1983) 1413.
[23] E.D. Palik, V.M. Bermudez and O.J. Glembocki, J. Electrochem. Soc. 132 (1985) 871.
[24] E.D. Palik, O.J. Glembocki and T. Heard, Jr., J. Electrochem. Soc. 134 (1987) 404.
[25] O.J. Glembocki, R.E. Stahlbush and M. Tomkiewicz, J. Electrochem. Soc. 132 (1985) 145.
[26] M. Grundner and R. Schulz, AIP Conf. Proc. 167 (1987) 329.
[27] P. Jakob and Y.J. Chabal, J. Chem. Phys. 95 (1991) 2897.
[28] H.E. Hessel, A. Feltz, M. Reiter, U. Memmert and R.J. Behm, Chem. Phys. Lett. 186 (1991) 275.
[29] G.S. Higashi, R.S. Becker, Y.J. Chabal and A.J. Becker, Appl. Phys. Lett. 58 (1991) 1656.

[30] R.S. Becker, G.S. Higashi, Y.J. Chabal and A.J. Becker, Phys. Rev. Lett. 65 (1990) 1917.
[31] J.A. Schaefer, F. Stucki, D.J. Frankel, W. Göpel and G.L. Lapeyre, J. Vac. Sci. Technol. B 2 (1984) 359.
[32] J.A. Schaefer, J. Anderson and G.L. Lapeyre, J. Vac. Sci. Technol. A 3 (1985) 1443.
[33] P. Allongue, V. Kieling and H. Gerischer, to be published.
[34] J. Koryta and J. Dvorak, in: Principles of Electrochemistry (Wiley, New York, 1987) p. 340.
[35] F.A. Cotton and G. Wilkinson, Advanced Inorganic Chemistry (Wiley, New York, 1980).
[36] D. Barton and W.D. Ollis, Comprehensive Organic Chemistry (Pergamon, Oxford, 1979).